ELSEVIER

Polymer 40 (1998) 253–259

polymer

Determination of Avrami exponent by differential scanning calorimetry for non-isothermal crystallization of polymers

Kim Piew Chuah, S. N. Gan, K. K. Chee*

Department of Chemistry, University of Malaya, 50603 Kuala Lumpur, Malaysia

Received 17 November 1997; revised 12 January 1998; accepted 12 February 1998

Abstract

A novel approach was developed to study the non-isothermal crystallization kinetics of polymers based on the Ozawa equation. The method determines the Avrami exponent, n, using exclusively the data confined to the primary crystallization regime. It was applied to a selection of eleven semicrystalline polymers including some biodegradable polyesters. The differential scanning calorimetry exotherms were obtained from the cooling rates covering 2 to 40 K min^{-1}. As noted, poly(-caprolactone) and nylon 6,10 resulted in the lowest and highest n, being equal to 1.5 and 5.1, respectively. The present findings on n were compared with those reported in the literature. Their morphological implications were also discussed.

Keywords: Ozawa equation; Crystallization kinetics; Semicrystalline polymers

1. Introduction

Bulk crystallization of a polymer would lead to various degrees of crystallinity, which might have profound effects on, among others, its thermal, mechanical and optical properties. A number of theories were proposed to rationalize the kinetics of this important transformation phenomenon [1]a, providing insight into the underlying molecular processes and the resulting morphology. For example, Avrami has derived an equation for the isothermal crystallization kinetics expressed in terms of the time dependence of the volume fraction of crystalline material, X_v, by considering the rates of nucleation and volume increase in lamellar crystals as the major kinetic events [2]. This particular model is characterized by two parameters including the Avrami exponent, n, which is susceptible to the crystallization mechanism.

Although the Avrami equation is applied extensively in studying the polymer crystallization behaviour under isothermal conditions, it is rather irrelevant to most polymer processing operations, such as the injection-molding process which usually involves rapid quenching of molten polymers. This situation was envisaged by Ozawa, who extended the Avrami model to the non-isothermal crystallization conditions [3] depicted by:

$$X_v = 1 - \exp(-f_c/q^n) \quad (1)$$

where f_c is the cooling crystallization function and q is the cooling rate. Eq. (1) was successfully applied to determine the exponent n, which is assumed to be temperature-independent, for some semicrystalline polymers [3–5] by taking f_c as a constant at a designated temperature, T. Apparently, only a limited number of X_v data are available for the foregoing analysis, designated as method A hereafter, as the onset of crystallization varies considerably with the cooling rate. In addition, the equation is valid exclusively for primary crystallization before crystal growth impingement takes place at high transformation.

Recently, Caze et al. [6] have assumed an exponential increase of f_c with T upon cooling. On this basis, the temperatures at the peak and the two inflection points of the exotherm with skew Gaussian shape are linearly related to $\ln q$ in order to estimate the exponent n. However, this treatment, designated as method B hereafter, seems to hold only for $q < 10$ K min^{-1} for unfilled and filled polypropylene (PP), because of the superposition of crystallization regimes 1 and 2 at higher q.

The main objective of this study is to overcome the inadequacies of methods A and B for the same purpose. To this end, the crystallization behaviour of four distinct classes of

* Corresponding author.

0032-3861/98/$ - see front matter
PII: S0032-3861(98)00188-8

semicrystalline polymers including polyhydrocarbons, polyoxides, polyamides and biodegradable polyesters are studied by differential scanning calorimetry (DSC).

2. The method

By means of integrating the partial areas under the DSC endotherm, one would obtain the values of the crystalline weight fraction X_w. Now X_v is accessible by:

$$X_v = X_w(\rho_a/\rho_c)[1-(1-\rho_a/\rho_c)X_w]^{-1} \quad (2)$$

where ρ_a and ρ_c are the bulk densities of the polymer in the amorphous and pure crystalline states, respectively. In order to account for the T effects on the ratio ρ_a/ρ_c, we resort to the empirical rules after Boyer–Spencer and Bondi [7], respectively given by $\alpha_a T_g = 0.16$ and $\alpha_c T_m^\circ = 0.11$, where α_a and α_c are the thermal expansion coefficients of the polymer in the amorphous and crystalline states, respectively with their respective glass transition temperature T_g and equilibrium melting point T_m°. As a result, we have:

$$\rho_a/\rho_c = (\rho_{ao}/\rho_{co})\exp[(T-T_r)(0.11/T_m^\circ - 0.16/T_g)] \quad (3)$$

where the second subscript 'o' refers to the reference temperature T_r taken as 298 K in this case.

On the basis of the findings on the crystallization behaviour of poly(ethylene terephthalate) (PET) and PP [3,4,6] we propose:

$$\ln f_c = a(T-T_1) \quad (4)$$

where a and T_1 are the empirical constants. If the extreme point of the pertinent $\partial X_v/\partial T$ curve occurs at $T = T_q$, i.e. $(\partial^2 X_v/\partial T^2)_{Tq} = 0$, we have [6]:

$$f_c(T_q) = q^n \quad (5)$$

Combining Eqs. (1), (4) and (5) yields:

$$\ln[-\ln(1-X_v)] = a(T-T_q) \quad (6)$$

Hence, a linear plot of $\ln[-\ln(1-X_v)]$ against T would result in the constant a and the product $-aT_q$ from the gradient and intercept, respectively. At $T = T_q$ obtained from the foregoing algorithm, Eqs. (4) and (5) lead to:

$$T_q = n\ln q/a + T_1 \quad (7)$$

Clearly, T_1 is the T_q at q = 1 K min^{-1}. In fact, the Ozawa theory [3] has revealed that the quantity f_c is not only a function of undercooling but also the temperature at the onset of crystallization. This implies that the coefficient a in Eq. (4) is virtually q-dependent. As such, parameters n and T_1 are obtainable from the linear plot of T_q against $\ln q/a$ in accordance with Eq. (7).

3. Experimental

A total of eleven semicrystalline polymers was selected for the present study. They were listed in Table 1, together with their designations and suppliers. All materials are used as received.

Thermogravimetric analysis (TGA) of each polymer was carried out with a Rheometric TGA1000 + in N_2 at a heating rate of 20 K min^{-1}. Basically, it continuously monitors the sample weight as a function of T. Two points A and B are used to mark, respectively the start and the end of the catastrophic degradation process. The former is directly interpolated from a TGA trace at the point where the weight commences to drop rapidly, whereas the latter refers to the intersection of the tangent line to the curve and the terminal line where the curve tapers off. This would allow one to have facile access to the percentages of sample weight retained at A and B designated, respectively by W_i and W_f and their respective decomposition temperatures T_i and T_f.

DSC measurements were conducted with a Perkin–Elmer DSC7 system using N_2 as purge gas. The instrument was calibrated with indium standard for temperature and heat change. The non-equilibrium melting point, T_m, was derived from the peak temperature of the melting endotherm. A standard heating rate of 20 K min^{-1} was used for all the heating events unless specified otherwise. In a typical non-isothermal crystallization run, a sample weighing between 6.1 to 9.5 mg was first heated to an annealing

Table 1
Details of various polymers and their characterization by DSC and TGA

No.	Polymer designation	Supplier	(a)T_m K^{-1}	T_i K^{-1} (W_i/%)	T_f K^{-1} (W_f/%)
1	High density polyethylene (HDPE)	BDH	407.7 ± 1.1	723.9 (98.5)	826.9 (2.6)
2	Low density polyethylene (LDPE)	BDH	385.3 ± 0.4	590.4 (99.6)	818.6 (3.2)
3	Polypropylene (PP)	BDH	433.9 ± 0.9	617.0 (100.2)	808.4 (1.9)
4	Trans-polyisoprene (PIP)	Aldrich	330.9 ± 0.9	596.0 (99.2)	734.8 (0.7)
5	Polyoxymethylene (POM)	Aldrich	453.8 ± 1.4	545.0 (100.0)	714.1 (0.9)
6	Poly(ethylene oxide) (PEO)	Aldrich	341.7 ± 0.9	595.2 (101.5)	742.2 (3.9)
7	Poly(3-hydroxybutyric acid) (PHBA)	Aldrich	447.7 ± 0.6	551.3 (102.0)	611.3 (3.3)
8	Poly(ε-caprolactone) (PCL)	Aldrich	330.0 ± 1.4	637.3 (99.7)	766.2 (1.3)
9	Poly(ethylene terephthalate) (PET)	Aldrich	529.1 ± 2.3	685.7 (99.9)	790.7 (15.6)
10	Nylon 12 (N12), i.e. polydodecylamide	BDH	451.8 ± 0.2	718.5 (96.6)	819.0 (0.8)
11	Nylon 6,10 (N610), i.e. poly-(hexamethylene sebacamide)	BDH	495.4 ± 0.7	699.8 (96.5)	828.4 (1.8)

(a) The heating rate for all polymers was 20 K min^{-1} except for numbers 7, 8 and 9, which were heated at 40 K min^{-1}

temperature, T_a, above its melting point, and held at the molten state for at least 5 min (Table 3), before it was cooled with a constant rate, q, to record the exotherm. These heating and cooling steps were repeated continuously to cover various cooling rates with the same sample.

All linear regression analyses were performed with a personal computer software.

4. Results and discussion

Typical DSC and TGA thermograms pertaining to the heating mode are shown in Fig. 1, which exhibits the T_m, and the thermal decomposition profile for PEO. The foregoing parameter serves as an indicator for the approximate molecular size of the polymer, which may affect the rate of crystallization [8]. Whereas the one-step decomposition curve in Fig. 1(*b*) characterized by the points A and B, would register the purity of the sample. Here, the values of W_i, W_f, T_i and T_f are reported. The present work concerns with the final residue at T_f, because it may function as an active nucleation agent. Table 1 shows the data thus obtained for the polymers studied.

Conventional technique was resorted to for estimating the crystalline weight fraction X_w at various undercoolings from the DSC exotherms [9]. Eqs. (2) and (3) facilitate the conversion of X_w to X_v with the aid of the pertinent literature data [10–17] displayed in Table 2. This would allow one to display the non-isothermal crystallization kinetics by plotting X_v against T as shown in Fig. 2(*a*) for a biodegradable

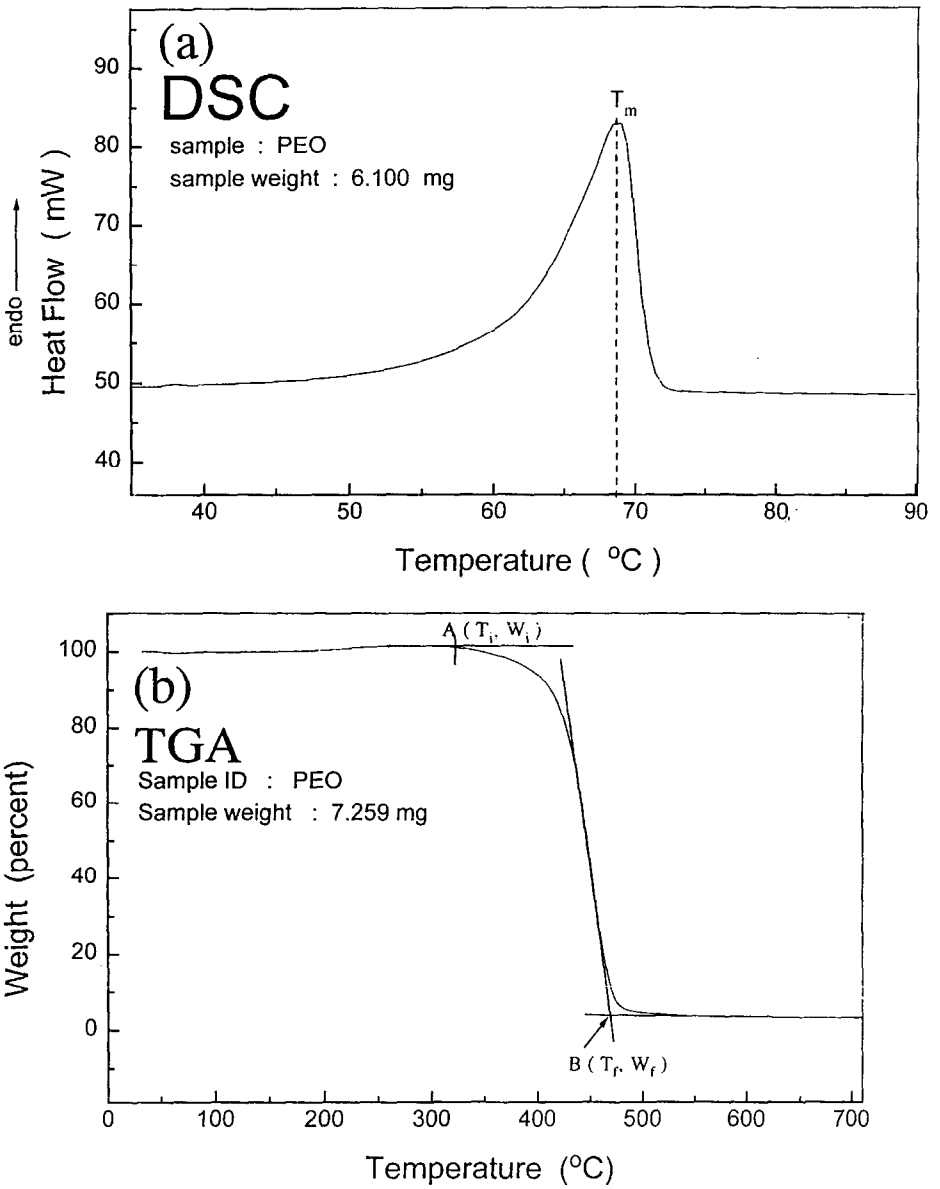

Fig. 1. (a) DSC melting endotherm, and (b) TGA thermogram for PEO, characterized by T_m, and A (T_i, W_i), $B(T_f, W_f)$, respectively. In this case, heating rate, q = 20 K min^{-1}, and $T_m = 68.7°C$, $T_i = 322.0°C$, $T_f = 469.0°C$, $W_i = 101.5\%$, and $W_f = 3.9\%$

Table 2
Thermal characteristics of various polymers from the literature

No.	Polymer	Density at 25°C		Transition temperature		Ref.
		ρ_{ao} g^{-1} ml^{-1}	ρ_{co} g^{-1} ml^{-1}	T_g K^{-1}	T_m° K^{-1}	
1	HDPE	0.855	1.00	153	414.2	[10a][11]
2	LDPE	0.855	1.00	140	386.2	[10a]
3	PP	0.85	0.936	256.2	444.2	[10a]
4	PIP	0.905	1.05	207.0	338.2	[10b,c]
5	POM	1.251	1.494	191.0	454.2	[10d]
6	PEO	1.125	1.33	213.2	348.0	[12,13]
7	PHBA	1.177	1.260	277.2	453.2	[14,15]
8	PCL	1.09	1.185	212.7	332.3	[16,17]
9	PET	1.335	1.501	340.2	553.2	[10e]
10	N12	1.01	1.04	314.0	460.2	[10f]
11	N610	1.05	1.09	323.0	488.2	[10f]

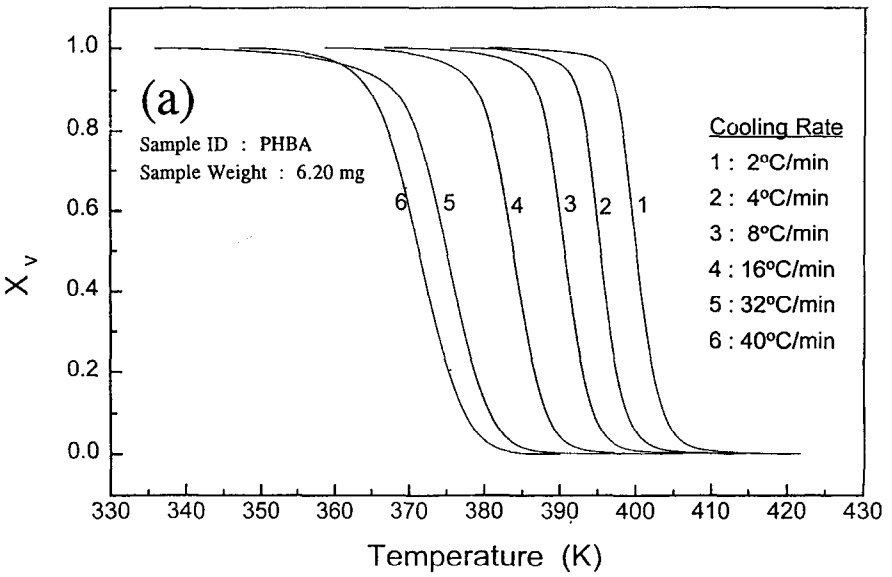

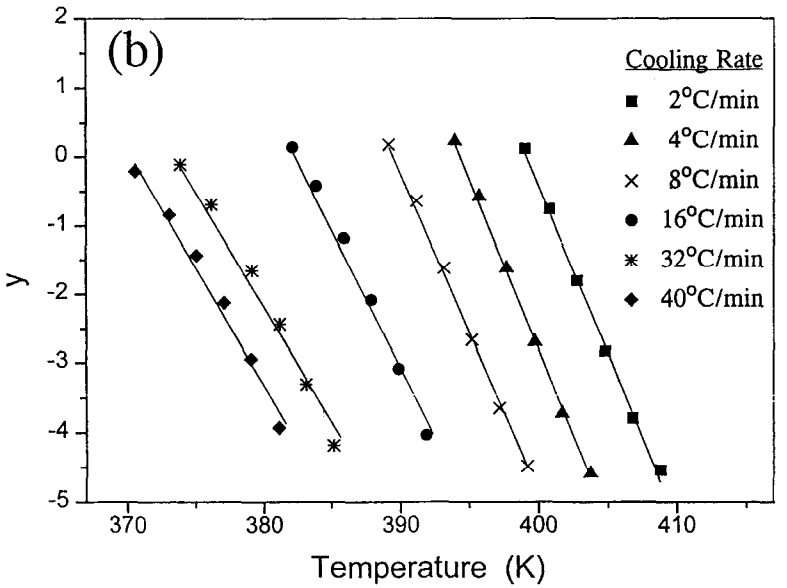

Fig. 2. Dynamic crystallization behaviour of PHBA: (a) plots of X_v against T, (b) linear plots of $y = ln\ [-\ln(1 - X_v)]$ against T. The cooling rates are 2, 4, 8, 6, 32 and 40 K min^{-1} for lines/curves 1–6, respectively

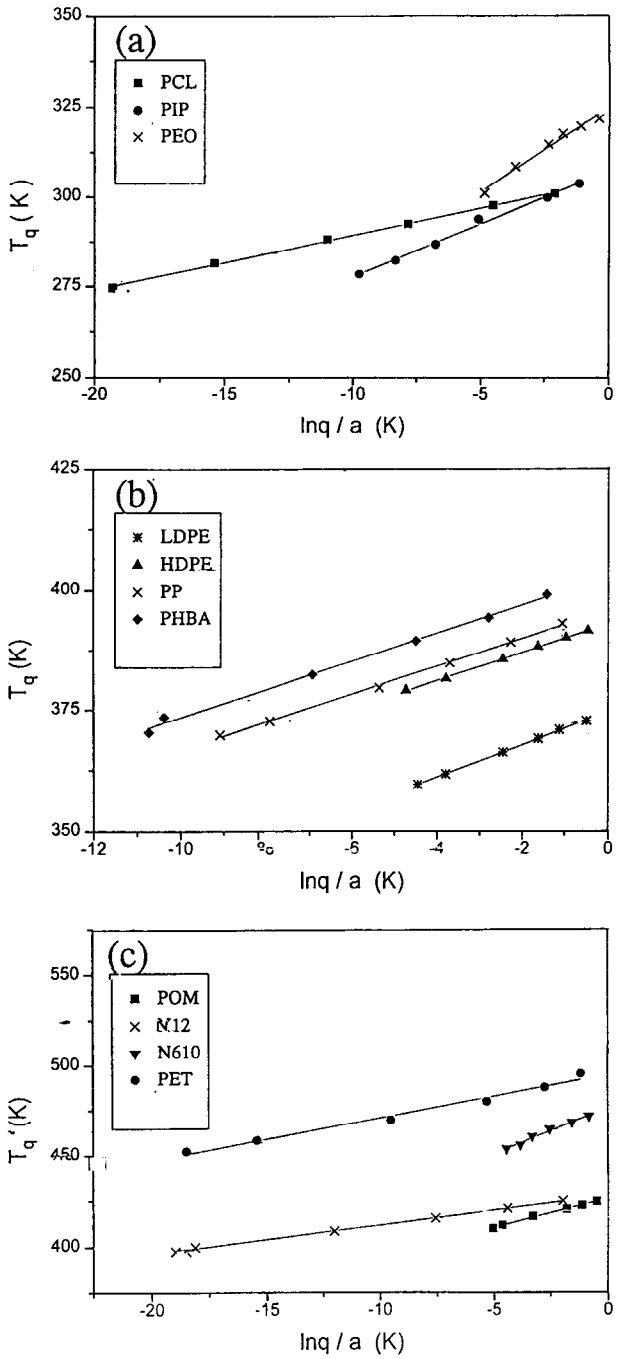

Fig. 3. Linear plots of T_q against ln q/a for various polymers: (a) PCL, PIP, PEO; (b) LDPE, HDPE, PP, PHBA; (c) POM, N12, N610, PET

polymer, PHBA. The cooling rates are 2, 4, 8, 16, 32 and 40 K min^{-1}. Fig. 3(*b*) exhibits the corresponding linear plots of ln [$-$ ln $(1 - X_v)$] against T, constructed according to Eq. (6) as to estimate the parameters a and T_q. The foregoing exercise was readily extended to other polymers.

According to the Ozawa Theory, Eq. (6) is virtually confined to the crystallization regime 1 [3,18]. As such, the foregoing linear regression analyses are made to comply with two criteria: (1) the lowest X_v employed is close to the onset of crystallization (i.e. $X_v = 0$) and kept between ca 1 to 2%, at which the relative precision in X_v is acceptable; and (2) the range of X_v selected covers the data which would result in the coefficient of determination $r^2 > 0.9800$ with r being the linear correlation coefficient. The latter warrants that any X_v data from the secondary crystallization, if included adventitiously, would have negligible impact on the results.

Our results disclose that the usable X_v-ranges do change appreciably with the cooling rate. This means that Eq. (6) is more adaptable to the variation of q than method A [3–5]. The values of T_q obtained refer to $X_v = 0.6321$, and are found to be lying outside the corresponding X_v-ranges from which they are based, for all the polymers except PP, PCL, PHBA and N12. This means that the present analysis does not rest on the observed T_q. However, method B hinges on the three temperatures including T_q derived graphically from the experimental exotherm as cited earlier, without justifying if they are truly within the permissible crystallization regime. In addition, the present findings show that the absolute a, i.e. $|a|$, increases with decreasing q. In contrast, method B treats this particular parameter as a constant with q.

Fig. 3 illustrates the linear plots of T_q against ln q/a for all the systems of interest. Here, the values of n and T_1 are obtained and collected in Table 3 which also displays the T_a. The lowest r^2 registered for the foregoing analyses is 0.9822, which corresponds to the highest relative standard deviation in n reported for PET.

The n values determined by the present approach, hereafter designated as method C, are compared with those cited in the literature [4,13,17,19–26] in Table 3. Our findings on the exponent n suggest that non-isothermal crystallizations of HDPE, LDPE, PP, PIP, POM and PHBA seem to proceed via heterogeneous nucleation and 3-dimensional spherulitic growth. Compatible observations are obtained from other sources based on the Avrami equation unless stated otherwise, for the four polyhydrocarbons except HDPE, whose n value cited is marginally lower as shown in Table 3. For PP, methods A and B yield $n = 2.79$ [4] and 3.3 [6], respectively. In fact, the former technique fails for HDPE by using cooling rates varying from 0.5 to 10 K min^{-1} [4]. However, Philip and Lambert [27] have concluded that $n = 2.93 \pm 0.12$ by monitoring the changes in the transmitted light intensity during the isothermal crystallization of this particular polyolefin. Both POM and PHBA were confirmed to crystallize below 431 K [28], and from 343.2 to 383.2 K [29], respectively to yield spherulitic morphology by means of optical microscopy. These findings are in agreement with the present results, but grossly contradict a value of $n \approx 2$, which rather infers mechanism of heterogenous nucleation and 2-directional growth. It is noted that some workers tend to ignore the importance of volume change on crystallization, which could introduce significant errors in the determination of n [1b].

Perhaps one of the polymers most extensively studied by Avrami equation is PEO. Here, the estimates of n reported by two different groups of workers [13,23] are distinctly

lower than ours. The large exponent n observed in the present work may be associated with the impurity of the sample, as the diluting effect of any low-molecular-weight molecules would promote segmental mobility and enhance crystallization rate. It is interesting to note that method C would render $n = 2.58 \pm 0.09$ using, instead the X_v range varying from 0.10 to 0.73, which is comparable with that of Cheng and Wunderlich [23]. However, this finding should merely be considered as a convenient representation of the crystallization data, as the foregoing analysis was unduly extended to regime 2.

De Juana et al. have reported $n = 3.0$ for PCL crystallizing isothermally at temperatures ranging from 308 to 321 K. However, at the higher undercoolings, this 3-directional crystal growth becomes diffusional-controlled, reducing the n value by half [30] as observed by method C.

The literature values of n reported for high molecular weight PET are rather variable including those resulting from method A [3], under various melting and crystallization conditions [25] as shown in Table 3. Time-resolved light-scattering studies on the morphology of PET by Lee et al. [31] have revealed that spherulite prevails throughout the course of crystallization. Table 3 shows that the present study offers a somewhat lower crystallization rate. The TGA thermogram indicates that our PET sample contains $\approx$ 16% (w/w) catalyst residue whose surface may be wetted by the melt. As a result, the chain mobility and subsequently the crystal growth rate are significantly retarded. The presence of additives in other samples as detected by TGA, was deemed to have no significant effects on their crystallization behaviour, unless stated otherwise, by virtue of their small proportions and inertness to the polymer melts.

Clearly, the most pronounced difference between the dynamic and quiescent crystallization kinetics is encountered for N12. The former yields a slower rate leading to $n = 1.5$ and fribillar morphology, whereas the latter generates a sheaf-like structure, probably as a result of the change of mechanism at the lower undercoolings [26]. Polyamide N610 exhibits the fastest rate of primary crystallization observed in this study, leading to $n = 5.1$. The overall temperature evolution of the degree of crystallinity is shown in Fig. 4, which illustrates the abrupt and drastic decrease in the crystallization rate caused by the impingement of crystal entities occurring at X_v slightly above 0.50.

The model of branching crystals proposed by Booth and Hay [32] has resulted in $n = 5$ for heterogeneous nucleation. This infers that the non-isothermal crystallization kinetics of PEO and N610 is governed by branching mechanisms leading to solid sheaves. Other systems reportedly exhibiting the parallel morphological features including cross-linked polyethylene [20], nylon 8, nylon 12, and poly(hexamethylene adipate) [1a].

5. Conclusion

The conventional treatment of the crystallization kinetic data based on Ozawa equation is modified by employing an empirical expression for the cooling crystallization function. As a result, the method is successfully applied to deal with a variety of polymers in determining the Avrami exponent varying from 1.5 to 5.0. These values are reproducible by the classical Avrami equation in many instances. Any discrepancies between the results from these two distinct equations can be primarily attributed to the differences in the thermal history, crystallization conditions, and sample impurity. However, precise interpretation of the exponent n is not possible without the complementary information on the morphology and crystallization mechanism. Despite this, the Ozawa equation is a useful tool for depicting the dynamic crystallization behaviour of polymers. More importantly, it provides a practical means of assessing the Avrami exponent reliably over a wide range of undercoolings.

Acknowledgements

The authors thank the PKSN of Malaysian Government

Table 3
Annealing temperature and characteristic parameters obtained from non-isothermal and isothermal crystallization kinetics of various polymers

No.	Polymer	(a) $T_a K^{-1}$	$T_1 k^{-1}$	$n \pm n^{(b)}$		
				This work	Literature	(Ref.)
1	HDPE	433	393.0	2.97 ± 0.04	2.35 ± 0.28	[19]
2	LDPE	423	374.5	3.33 ± 0.03	3.15 ± 0.04	[20]
3	PP	453	395.8	2.91 ± 0.06	2.78 ± 0.19	[4]
4	PIP	373	307.3	2.95 ± 0.12	2.60 ± 0.20	[21]
5	POM	483	426.0	3.13 ± 0.10	2	[22]
6	PEO	373	324.7	4.65 ± 0.30	2.63 ± 0.16	[13]
					2.60 ± 0.39	[23]
7	PHBA	458	402.9	2.95 ± 0.09	2.07 ± 0.12	[24]
8	PCL	353	304.4	1.51 ± 0.03	3.00 ± 0.10	[17]
9	PET	548	494.3	2.35 ± 0.16	3.2 ± 0.6	[25]
10	N12	463	427.5	1.57 ± 0.03	5.06 ± 0.33	[26]
11	N610	513	475.9	5.11 ± 0.31	—	

(a) The corresponding annealing time is 5 min for PHBA, PCL and PET, and 10 min for all the other polymers; (b) standard deviation of n

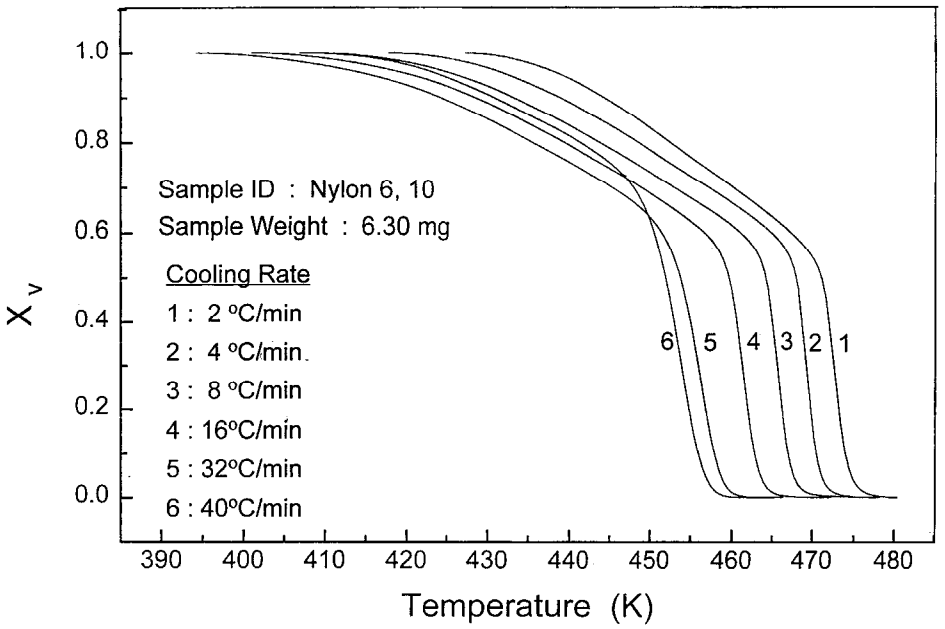

Fig. 4. Plots of X_v against T for N610. The cooling rates are as in Fig. 2

for financial support under the research fund R and D 09-02-03-0022.

References

[1] Wunderlich B. Macromolecular Physics, vol. 2, Academic Press, New York, (a) chapters 5 and (b) 6; pp. 139–141, 1976.
[2] Avrami M. Journal of Chemistry Physics 1941;9:177.
[3] Ozawa T. Polymer 1971;12:150.
[4] Eder M, Wlochowicz A. Polymer 1983;24:1593.
[5] Lopez LC, Wilkes G. Polymer 1989;30:882.
[6] Caze C, Devaux E, Crespy A, Cavrot JP. Polymer 1997;38:497.
[7] van Krevelen DW, Hoftyzer PJ. Properties of Polymers. Elsevier Scientific Publishing Company, Amsterdam, p. 68, 1976.
[8] Wunderlich B. Macromolecular Physics, vol. 3. Academic Press, New York, p. 79, 1980.
[9] Cira PJ, Magill JH. Macromolecules 1990;23:2350.
[10] (a) Quirk, RP, Alsamarraic AA. p. V/15; (b) Peyser P. p. VI/209; (c) Miller RL. p. VI/1; (d) Sexto G. p. V/87; (e) Lawton E, Ringwald EL. p. V/101; (f) Pfliiger R. p. V/109, in Bandrup J, Immergut EH. Eds Polymer Handbook, 3rd ed Wiley–Interscience, New York, 1989.
[11] Alamo RG, Viers BD, Mandelkera L. Macromolecules 1995;28:3205.
[12] van Kremelen DW, Hoftzer PJ. Properties of Polymers. Elsevier Scientific Publishing Company, Amsterdam, p. 574, 1976.
[13] Martuscelli E, Pracella M, Yue WP. Polymer 1984;25:1097.
[14] Doi Y. Microbial Polyesters. VCH Publishers, New York, p. 1011, 1990.
[15] Azuma Y, Yoshie N, Sakurai M, Inoue Y, Chujo R. Polymer 1992;33:4763.
[16] Cheung YW, Stein RS, Wignall GD, Yang HE. Macromolecules 1993;26:5365.
[17] de Juana R, Cortazer M. Macromolecules 1993;26:1170.
[18] Perez-cardenas FC, del Caslillo LF, Vera-Graziano R. Journal of Applied Polymer Science 1991;43:779.
[19] Hoffman DM, Mckinley BM. Polymer Engineering Science 1985;25:562.
[20] Phillips PJ, Kao YH. Polymer 1986;27:1679.
[21] Godovsky YK, Slonimsky GL. Journal of Polymer Science Polymer Phys Ed 1974;12:1053.
[22] Inoue M, Takayanyi T. Journal of Polymer Science 1960;47:498.
[23] Cheng SZD, Wunderlich B. Journal of Polymer Science Polymer Phys Ed 1986;24:595.
[24] Pagliu D, Beltrame PL, Canetti M, Seves A, Marcandalli B, Martuselli E. Polymer 1993;34:996.
[25] Vilanova PC, Ribas SM, Gazman GM. Polymer 1985;26:423.
[26] Maneschalchi F, Rossi R, Mathusi A. European Polymer Journal 1973;9:601.
[27] Philips PJ, Lambert WS. Macromolecules 1990;23:2075.
[28] Pelzbauer A, Galeski A. Journal of Polymer Science, Part C 1972;38:23.
[29] Xing P, Dong L, An Y, Feng Z, Avella M, Martuscelli E. Macromolecules 1997;30:2726.
[30] Cheng SZD, Wunderlich E. Macromolecules 1988;21:3327.
[31] Lee CH, Saito H, Inoue T. Macromolecules 1993;26:6566.
[32] Booth A, Hay JN. British Polymer Journal 1972;4:9.